Neuropsychologia 191 (2023) 108703

Contents lists available at ScienceDirect

Neuropsychologia

journal homepage: www.elsevier.com/locate/neuropsychologia

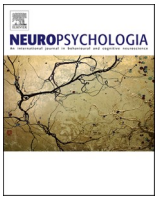

Characterising modulatory effects of high-intensity high frequency transcranial random noise stimulation using the perceptual template model

Efstathia Stephanie Gotsis [a,*], Jeroen J.A. van Boxtel [b], Christoph Teufel [c], Mark Edwards [a], Bruce K. Christensen [a]

[a] The Australian National University, Canberra, ACT, Australia
[b] University of Canberra, Canberra, ACT, Australia
[c] Cardiff University, Cardiff, Wales, United Kingdom

ARTICLE INFO

Keywords:
Early visual perception
Internal neural noise
Perceptual template model
Transcranial random noise stimulation

ABSTRACT

Neural noise is an inherent property of all nervous systems. However, our understanding of the mechanisms by which noise influences perception is still limited. To elucidate this relationship, we require techniques that can safely modulate noise in humans. Transcranial random noise stimulation (tRNS) has been proposed to induce noise into cortical processing areas according to the principles of stochastic resonance (SR). Specifically, it has been demonstrated that small to moderate intensities of noise improve performance. To date, however, high intensity tRNS effects on neural noise levels have not been directly quantified, nor have the detrimental effects proposed by SR been demonstrated in early visual function. Here, we applied 3 mA high-frequency tRNS to primary visual cortex during an orientation-discrimination task across increasing external noise levels and used the Perceptual Template Model to quantify the mechanisms by which noise changes perceptual performance in healthy observers. Results show that, at a group level, high-intensity tRNS worsened perceptual performance. Our computational analysis reveals that this change in performance was underpinned by an increased amount of additive noise and a reduced ability to filter external noise compared to sham stimulation. Interestingly, while most observers experienced detrimental effects, a subset of participants demonstrated improved performance. Preliminary evidence suggests that differences in baseline internal noise levels might account for these individual differences. Together, these results refine our understanding of the mechanisms underlying the influence of neural noise on perception and have important implications for the application of tRNS as a research tool.

1. Introduction

Neural noise is commonly described in terms of stochastic variability in neuronal firing, where systems with more noise will have greater variation in neuronal activity (Faisal et al., 2008; Homayoun and Moghaddam, 2007). An ongoing debate concerns the mechanisms by which neural noise affects perception, as causal links have not been clearly established. In the past decade, efforts have therefore been invested into the development of experimental techniques that can safely manipulate neural noise in the healthy brain, potentially providing tools to explore the effects of noise on perceptual performance more directly.

Transcranial random noise stimulation (tRNS) is a non-invasive electrical brain stimulation method shown to influence perceptual performance across several areas, including facial identification, perceptual learning, and perceptual decision-making (Contemori et al., 2019; Penton et al., 2018; Fertonani et al., 2015; van der Groen et al., 2018). The mechanisms by which tRNS modulates brain function are not fully understood, but previous studies suggest that tRNS effects manifest via the modulation of internal neural noise according to stochastic resonance (SR; Antal and Herrmann, 2016; Fertonani and Miniussi, 2017; Miniussi et al., 2013; Ward, 2009). SR leads to a non-monotonic relationship between noise and perceptual performance in the shape of an inverted-U function (Aihara et al., 2010; Treviño et al., 2016; Raul et al., 2023). The non-monotonic dependence occurs for sub-threshold signals, when the addition of a small to moderate amount of neural noise pushes a weak signal above the threshold for excitation (Moss et al., 2004; McDonnell and Ward, 2011). For lower noise levels, the signal (plus noise) remains sub-threshold, while higher noise levels obscure the signal.

Van Der Groen and Wenderoth (2016) demonstrated tRNS influences resembling some of the effects predicted by SR. They applied

* Corresponding author. Research School of Psychology, Building 39, Science Road, The Australian National University, Acton, 2601, Canberra, ACT, Australia.
E-mail address: stephanie.gotsis@anu.edu.au (E.S. Gotsis).

https://doi.org/10.1016/j.neuropsychologia.2023.108703
Received 11 May 2023; Received in revised form 22 August 2023; Accepted 10 October 2023
Available online 18 October 2023

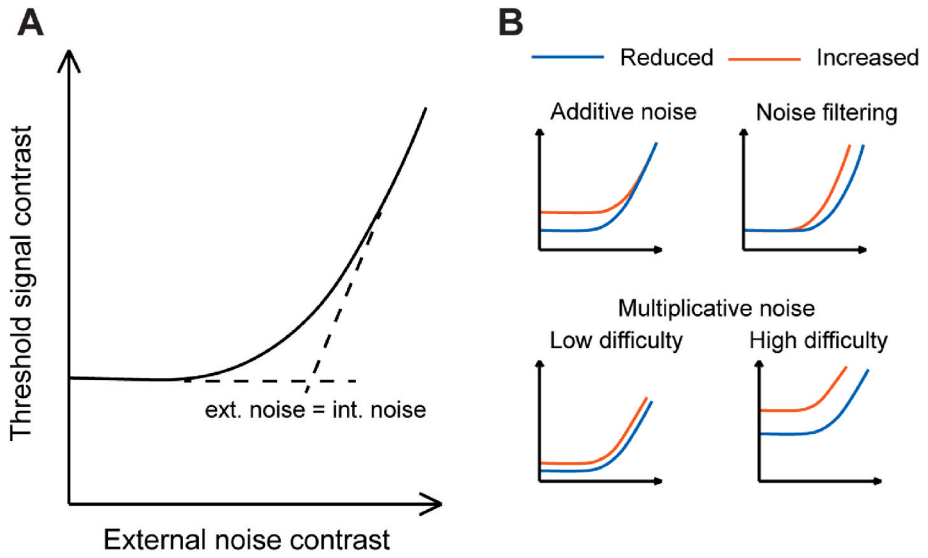

Fig. 1. Threshold versus noise contrast (TvN) function and PTM predictions.
Threshold signal contrast reflects the amount of contrast required to maintain a performance level (accuracy) as external noise is added to the stimulus. *A)* The TvN function is initially characterised by a flat slope in the presence of minimal external noise as performance is dominated by (largely constant) internal noise in the system. The addition of external noise has little to no effect on perceptual performance. As the external noise exceeds the internal noise amount, it impedes perceptual performance, leading to an increasing slope or 'arm' of the curve. The inflection indicates the point at which internal neural noise is equivalent to the external noise. *B)* The PTM predicts changes in TvN depending on the source(s) of noise that may vary (orange and blue curves indicate increased and reduced levels of noise, or increased and reduced impact on external noise filtering). Increased internal additive noise will increase thresholds across low levels of external noise (top left), while increased (i.e., worse) external noise filtering is demonstrated by increased thresholds at the arm of the curve (top right). Increasing internal multiplicative noise will increase thresholds across all external noise levels and have a greater ratio between thresholds at two different difficulty levels (bottom left and right).

high-frequency tRNS (101–640Hz; hf-tRNS) to the primary visual cortex (V1) in human participants during a visual detection task and found that moderate intensities of hf-tRNS (0.5 mA and 1 mA) led to improved performance, while a larger intensity (1.5 mA) resulted in perceptual performance comparable to baseline (0 mA). While these performance changes are consistent with SR, the principle not only predicts increased performance for moderate noise levels but also decreased performance for higher noise, which was not demonstrated. More importantly, no direct or computational measure was acquired to quantify neural noise levels, thus limiting the mechanistic insights that can be gained from this study. A more recent study (Potok et al., 2023) has also shown beneficial effects of moderate intensity hf-tRNS when applied to V1, but did not explore higher current intensities (i.e., >1.5 mA). Therefore, the extent to which high intensity hf-tRNS to V1 affects perception remains unclear. Hf-tRNS mechanisms on perception have been more extensively explored in motion processing (Ghin et al., 2018; Pavan et al., 2019; O'hare et al., 2021; Battaglini et al., 2023). These studies have similarly demonstrated that moderate intensities (i.e., 1 mA and 1.5 mA) of hf-tRNS applied to the medial temporal cortex (MT) can improve performance on global motion processing tasks. However, to date, only Pavan et al. (2019) have demonstrated a detrimental effect of hf-tRNS on perceptual performance by administering a larger than typical current intensity of 2.25 mA; although, this effect was not attributed to an increase in internal noise. Thus, overall, it is yet to be shown whether the high intensities of hf-tRNS can detrimentally impact perceptual performance by modulating internal noise.

The Perceptual Template Model (PTM) can be used to quantitatively estimate the intrinsic noise properties of observers. It assumes that visual function is determined by three noise-related factors: internal additive noise, internal multiplicative noise, and external noise filtering (Lu and Dosher, 2008). Internal additive noise most closely aligns with neural noise as typically discussed in the literature, reflecting noise in the system that is independent of the input and that underlies the stochastic and variable nature of internal responses. By contrast, internal multiplicative noise is dependent on the input and is analogous to contrast gain control mechanisms affecting the system's responsiveness to stimulus contrast. Lastly, external noise filtering reflects the perceptual system's inherent ability to separate relevant from irrelevant sensory information (Lu and Dosher, 2008). These three observer characteristics can be estimated by assessing visual function across different levels of external noise and fitting a computational model to the resulting threshold versus external noise contrast (TvN) function (Lu and Dosher, 2008, Fig. 1).

We therefore aimed to investigate if hf-tRNS could detrimentally impact contrast detection. We used intermittent 3 mA hf-tRNS, where stimulation was stimulus-locked, and the PTM to computationally quantify internal additive noise, internal multiplicative noise, and external noise filtering levels. We hypothesised that perceptual performance should be negatively affected by hf-tRNS via an increase in internal additive noise. Furthermore, we expected no improvement in the participants' ability to filter external noise given that our protocol avoided potential contamination by adaptation.[1] In fact, if continuous exposure to hf-tRNS is linked with adaptation to external noise we predicted that external noise filtering may even be negatively affected by the intermittent nature of our manipulation. Finally, we expected no effects of hf-tRNS on multiplicative noise.[2]

2. Material and methods

2.1. Participants

Forty-one healthy observers with normal or corrected-to-normal vision served as participants. All participants met the standard safety-

[1] It is clear that external 'visual' noise acts on perception according to SR, where small amounts can improve performance, while large amounts reduce performance (Van Der Groen and Wenderoth, 2016). Additionally, continuous exposure to external 'visual' noise can lead to noise adaptation, and consequently, improved perceptual performance (Menzel et al., 2017). Therefore, we suggest that if hf-tRNS also acts on perception according to SR, the presence of continuous hf-tRNS may also lead to noise adaptation.

[2] There is no previous research to suggest that we would expect to see a multiplicative effect.

related inclusion criteria for tRNS and were exposed to both sham (0 mA) and active (3 mA) tRNS conditions. The average participation duration was 2-h, and participants received university course credits or payment as remuneration. Participants were required to complete a tRNS safety questionnaire to determine their eligibility to participate in this study. Participants were excluded from participating if they identified any contraindications that would place them at a higher risk of experiencing negative side effects (e.g., metal implant in head). This study was approved by an Australian university Human Research Ethics Committee (2018/559), and informed written consent was obtained from all participants prior to commencing the experiment. Participants were aged between 18 and 33 years old ($M = 21.46$, $SD = 3.71$), and were primarily female (~73%).

2.2. Apparatus and stimuli

All computer-based tasks took place in a quiet and dark room. Visual stimuli were generated using Matlab version R2013b and the Psychtoolbox extensions (Brainard, 1997; Kleiner et al., 2007; Pelli and Vision, 1997). Stimuli were presented on a Compaq colour monitor (P1220) with a calibrated linearized output at a resolution of 1280 × 1024 pixels, and a refresh rate of 85Hz. A 14-Bit grayscale resolution was achieved using the Bits# Stimulus Processor (Cambridge Research Systems). Chin rest fixed the viewing distance at 60 cm, with each pixel subtending 0.028 deg of visual angle. The signal stimulus was a Gabor patch (spatial frequency $f = 4$ c/deg, Gaussian envelope $\sigma = 0.25$ deg) with a cardinal orientation (vertical or horizontal; $\theta = 0$ deg or 90 deg) presented in the centre of the screen. The background luminance (l_0) was 25 cd/m^2, the contrast of the Gabor patch was determined for every trial by the Psi method (see details below).

The signal Gabor patch was temporally sandwiched between two independent external noise samples (Fig. 2A). The noise samples had an identical Gaussian envelope to the signal Gabor patch and were constructed using 4 × 4 pixel elements and sampled from a Gaussian distribution with a mean of 0 and standard deviation of 0, 0.02, 0.04, 0.08, 0.12, 0.16, 0.25, and 0.33 (Fig. 2B).

2.3. Procedure and design

A two-alternative forced choice (2-AFC) task required participants to judge if the Gabor stimulus had a vertical or horizontal orientation (Fig. 2A) by pressing keys 1 or 2 on a keyboard numeric keypad. A 20 trial practice session that was identical to the main task was used to familiarise observers with the experiment. Ten practice trials were initially presented in the absence of external noise (0% noise standard deviation), while the remaining 10 practice trials were presented in the presence of high external noise (50% noise standard deviation). During the main experiment, the two experimental sessions (sham-tRNS and active-tRNS) were counterbalanced and used the Psi method to determine the stimulus contrast on every trial (Palamedes toolbox; Prins and Kingdon, 2009, Fig. 2C). Data to estimate psychometric functions for eight external noise conditions were acquired, using an interleaved design of 60 trials per noise condition. In total, 480 trials over 10 blocks containing 48 trials were completed. Between each block, participants were required to take a minimum 60 s break before proceeding. Weibull functions were used to estimate contrast thresholds for three different performance levels (d': 0.78, 1.35, and 2.07), corresponding to 65%, 75% and 85% performance accuracy:

$$P(c) = 1 - (1 - 0.5) \times 2^{-\left(\frac{\log(c)}{\alpha}\right)^{\eta}} \quad (1)$$

where the P is the percent correct, c is the stimulus contrast, α is the threshold parameter, and η is the slope parameter of the psychometric function.

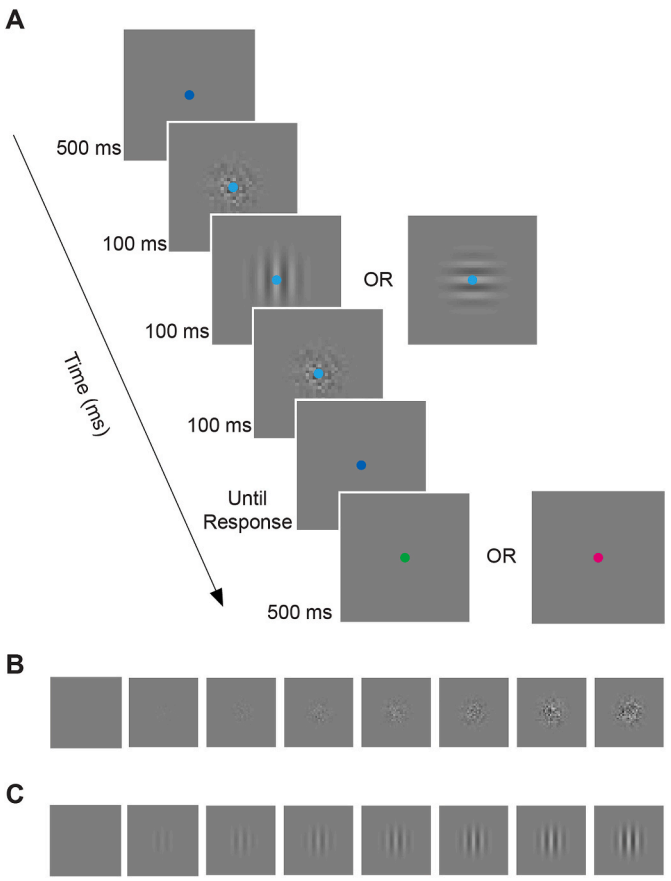

Fig. 2. Psychophysical task and features
A) Each trial began with a central dark-blue fixation dot. The stimulus sequence coincided with a fixation colour change to light-blue, and comprised a series of three frames: Gaussian pixel noise, oriented Gabor patch (vertical or horizontal), Gaussian pixel noise. Participants were asked o judge whether the grating was vertically or horizontally oriented. Feedback was provided in the form of a fixation colour change to green (i.e., correct) or red (i.e., incorrect) responses. From left to right: *B)* eight external noise images with increasing external noise (standard deviation: 0%, 2%, 4%, 8%, 12%, 16%, 25%, and 33%); *C*, a horizontally oriented signal Gabor patch with increasing contrast.

2.4. tRNS protocol

Participants received an active-tRNS current (3 mA) during one of the experimental sessions (active session), and sham-tRNS (0 mA) in the other (sham session). Stimulation was administered by a battery driven stimulator (Neurocare DC-Stimulator PLUS; https://www.neurocare group.com/technology/dc-stimulator-plus) through two 5 × 7 cm (i.e., 35 cm^2) electrodes were positioned on the participant's scalp and held in place with a soft rubber headband. The current density for 3 mA tRNS delivered across a 35 cm^2 electrode area was determined to be 0.0857 mA/cm^2; a value that lies well within the range of current densities for experiments showing no adverse effects (i.e., 0.040–0.167 mA/cm^2; Fertonani et al., 2015). The electrodes were coated with an electrode gel (Signa gel; Parker Laboratories Inc) to reduce skin impedance. Based on the 10–20 EEG system, the anode was positioned at the occipital region Oz and the cathode at the vertex of the scalp (Cz). This setup is an established method for stimulation of the primary visual cortex (Neuling et al., 2012; Van Der Groen and Wenderoth, 2016).

During the active session, 3 mA of high-frequency tRNS (hf-tRNS; 101–640Hz) was administered to participants during the task and terminated during breaks between blocks. Investigations applying such *intermittent* stimulation could be used to minimise the possibility of adaptation (Van Der Groen and Wenderoth, 2016). Stimulation was triggered by a spacebar press required to start each block and stopped at

the end of each block or after a maximum of 105 s (including a ramp-up stimulation phase of 5 s). The impedance of each electrode was checked before and during stimulation to ensure it was under 10 kΩ. The stimulation equipment set-up for sham-sessions was identical to the active-session, however no current (0 mA) was presented.

2.5. Perceptual template model analysis

The effects of stimulation on perceptual performance were estimated by fitting data of individual observers with the PTM and comparing active-tRNS versus sham-tRNS (implemented using Matlab version R2013b; See Appendix A, Table A-1 for individual PTM data). The PTM model provides a computational means to quantify the extent to which perceptual performance under each condition was limited by internal additive noise, internal multiplicative noise, or external noise filtering. The PTM models thresholds (c_τ) by equation (2) (Lu and Dosher, 2008):

$$c_\tau = \frac{1}{\beta}\left[\frac{\left(1+N_{mul}^2\right)N_{ext}^{2\gamma}+N_{add}^2}{\left(1/d'^2-N_{mul}^2\right)}\right]^{\frac{1}{2\gamma}}, \tag{2}$$

where each N refers to the variance of a normally distributed random variable with a mean of 0 for each respective noise type. An input consisting of signal and external noise (N_{ext}) is received by an observer and transformed into an internal representation. This representation is passed through a perceptual 'template', which can be understood as a filter with selectivity for certain visual characteristics. The system's ability to filter external noise will affect its ability to match the signal with the template. The signal can be enhanced by a gain factor β depending on how well the input is matched to the template. This template output will undergo another transformation through a nonlinear transducer function γ, accounting for the nonlinear properties of the visual system. Two sources of internal noise, that is additive (N_{add}) and multiplicative (N_{mul}), are added to the transformed signal.

tRNS effects were characterised by introducing three coefficient indices (*Aa(stim), Am(stim), and Af(stim)*) to the conventional equation (2). As seen in equation (3), each coefficient is multiplied by the corresponding source of noise: additive noise (N_{add}), multiplicative noise (N_{mul}), or external noise (N_{ext}):

$$c_\tau = \frac{1}{\beta}\left[\frac{\left(1+(A_m(stim)N_{mul})^2\right)\left(A_f(stim)N_{ext}\right)^{2\gamma}+(A_a(stim)N_{add})^2}{\left(1/d'^2-(A_m(stim)N_{mul})^2\right)}\right]^{\frac{1}{2\gamma}} \tag{3}$$

The influence of these noise types on performance between sham and active-tRNS conditions was determined by fixing sham stimulation coefficient indices (*Aa(sham), Am(sham),* and *Af(sham)*) to 1, while the indices for active stimulation (*Aa(active), Am(active),* and *Af(active)*) were free to vary. The resulting coefficients, therefore, describe the relative difference in the effects of tRNS between the stimulation groups; i.e., parameters greater than 1 suggest that the active stimulation produced higher amounts of the respective noise types compared to the sham stimulation. Eight forms of the PTM were considered on the basis that the coefficient indices for active stimulation could vary or be fixed to 1. For instance, a null model assumes that there are no group differences between stimulation conditions and, therefore, four free parameters (N_{mul}, N_{add}, β, and γ). Alternatively, the fullest model has up to seven free parameters.

The weight of each threshold data point fit by the PTM varied according to the goodness of fit (R^2) of the Weibull function used to obtain the threshold estimate. Weibull function fits that were <0.001 were set to 0.001 as a minimum, and weights were then normalised relative to the maximum threshold. Thus, threshold estimates with better fitting Weibull functions were weighted more heavily, compared to those obtained from poorer fitting functions. This ensured that the most reliable threshold estimates had the most influence in the model.

A least square procedure was used to fit the PTM to the TvN data for each participant. The least square difference between the log of the measured threshold contrast and the log of the model-predicted threshold contrast was minimised to find the best fit for the reduced and full models. The r^2 statistic was used to measure the PTM goodness-of-fit using equation (4):

$$r^2 = 1.0 - \frac{\Sigma\left[\log\left(c_\tau^{theory}\right)-\log(c_\tau)\right]^2}{\Sigma[\log(c_\tau)-mean(\log(c_\tau))]^2}, \tag{4}$$

where, Σ and *mean()* were applied across all external noise levels, stimulation conditions, and performance levels.

2.6. Akaike information criterion model selection

The best-fitting PTM was determined across participants by comparing the akaike information criterion (AIC; Wagenmakers and Farrell, 2004) for all eight PTM variations

$$AIC_i = 2k - 2\ln\left(\widehat{L}\right) \tag{5}$$

where k refers to the number of estimated parameters in the given model (i), and $\widehat{L}$ is the maximum value of the likelihood function for the model seen in equation (5).

The AIC for each model was calculated for individual participants and averaged (see Appendix B, Table B-1 for extended data). Specifically, the AIC analysis used the average error associated with the PTM full model (i.e., active stimulation) relative to the reduced model (i.e., sham) that was used to generate noise estimates for each PTM variation. Therefore, the best-fitting model identified by the AIC analysis not only indicates which model (i.e., combination of PTM noise parameters) best explain our data, but this also allows us to interpret differences between sham and active stimulation conditions between models. For instance, the PTM null model has the assumption that there are no differences between sham and active stimulation conditions (i.e., groups do not vary according to any PTM noise parameters). Therefore, if the AIC identifies that another model (e.g., including the additive noise parameter) meaningfully deviates from the null model, this indicates that changes in the noise parameters in that model drive differences between sham and active stimulation conditions.[3]

The model with a) the lowest AIC estimate, which b) meaningfully deviated from the other models (i.e., a difference greater than 2), was identified as having the best fit (Wagenmakers and Farrell, 2004). The differences in AIC with respect to the best-fit candidate model were calculated by equation (6):

$$\Delta AIC_i = AIC_i - minAIC \tag{6}$$

Akaike weights were then calculated to determine the relative strength of evidence in favour of this model over the other candidate models by equation (7):

$$w_i(AIC) = \frac{\exp\left\{-\frac{1}{2}\Delta AIC_i\right\}}{\sum exp\left\{-\frac{1}{2}\Delta AIC_k\right\}} \tag{7}$$

where the terms in equation (7) are proportional to the likelihood of the model. That is, the weight of a given model, $w_i(AIC)$, is equal to the relative likelihood of that model (numerator in equation (7)), divided by the sum of the relative likelihoods of all models (denominator in equation (7)) (Wagenmakers and Farrell, 2004). An evidence-ratio then

[3] We recognise that it is recommended for studies with smaller sample sizes (such as the present study) to implement a correction in the AIC to account for over fitting the model (Wagenmakers and Farrell, 2004). We performed the analysis with and without the correction (AICc), noting no difference to overal results (see supplementary material, Table 3). Therefore, we report the results of the AIC in the subsequent results section.

allowed us to infer how likely the best-fit model ($w_i(AIC)$) identified by the raw AIC values was over the next-best model ($w_j(AIC)$) using equation (8):

$$ratio = \frac{w_i(AIC)}{w_j(AIC)} \quad (8)$$

3. Results

3.1. Screening

Upon inspection of the PTM results for each participant ($N = 41$), we identified 6 participants whose data could not be fit by the PTM to a moderate or high standard (i.e., $r^2 < 0.5$) (Moore et al., 2013). As a result, data for these participants were excluded from analyses, leaving 35 participants in the final analysis.

3.2. AIC model selection

AIC model selection was applied to identify which of the eight PTM variations best accounted for differences between stimulation conditions. The PTM variation that included internal additive noise and external noise filtering (but not multiplicative noise) was identified as the best model (i.e., model AF; Table 1). This suggests that 3 mA hf-tRNS differed from sham-tRNS in levels of internal additive noise and external noise filtering produced, but not in the amount of internal multiplicative noise produced. An assessment of AIC weights (w(AIC); Table 1) further supports this conclusion, where model AF, accounted for approximately 31% of the total explanation that can be found in the full set of models.

Although the model consisting of external noise filtering only (i.e., model F) did not meaningfully deviate from model AF, further investigations of individual participant data supported the conclusion that model AFshould be considered as the best fitting model (see extended data in Appendix B Tables B-1 and B-2). Specifically, when model F had the best fit it did not meaningfully differ from model AF. However, when model AF had the best fit, it meaningfully differed to model F. Furthermore, when the null model had the best fit, model F did not meaningfully differ, but model AF did. Taken together, individual participant evaluations demonstrate that model AF should be favoured as the best fitting model to apply to our group data.

3.3. Best fitting PTM

Further investigations of the best fitting PTM demonstrated characteristic nonlinear TvN functions, where contrast thresholds increased as a function of increasing levels of external noise contrast (Fig. 3A). Internal additive noise estimates showed an average 19% increase under 3 mA hf-tRNS conditions compared to sham-tRNS (Fig. 3B). This effect is demonstrated in the TvN function by the increase in contrast threshold

Table 1
Akaike Information Criterion (AIC) estimated for PTM parameter combinations.

	Model Parameter Combinations							
	AFM	AF	AM	FM	A	F	M	Null
AIC	−38.19	−40.17	−35.99	−38.17	−36.80	−39.90	−36.00	−36.55
ΔAIC	1.98	0.00	4.17	1.99	3.37	0.27	4.17	3.62
w(AIC)	0.12	0.31	0.04	0.11	0.06	0.27	0.04	0.05

Note. The best fitting model has the smallest AIC estimate that meaningfully deviates from other models by a value of ~2 or more (ΔAIC is the difference between the best model and each other model); w(AIC) = AIC weight is proportional to the total amount of predictive power provided by the full set of models contained in the model being assessed (Wagenmakers and Farrell, 2004). AFM – fullest model with Aa, Af, and Am coefficients free to vary; AF – Aa and Af coefficients free to vary; AM – Aa and Am coefficients free to vary; FM – Af and Am coefficients free to vary; A – Aa coefficient free to vary; F – Af coefficient free to vary; M – Am coefficient free to vary; Null – Aa, Af, and Am fixed to 1.

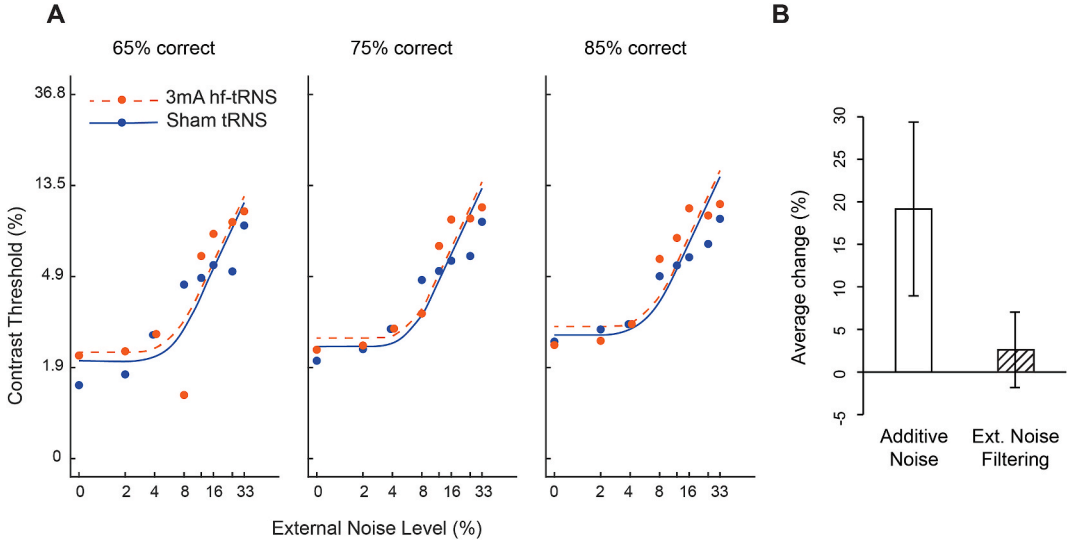

Fig. 3. Contrast threshold versus external noise contrast (TvN) functions and changes in noise.
A) TvC functions at for a representative participant showing 65% (left panel), 75% (middle panel), and 85% (right panel) performance accuracy. This representative participant reflects the average findings, displaying ~20% increase in additive noise and ~3% increase in external noise filtering under 3 mA hf-tRNS (orange circle + dashed line) compared to sham (blue circle + solid line) estimated by the PTM. Eight external noise levels (standard deviation: 0%, 2%, 4%, 8%, 12%, 16%, 25%, and 33%). *B)* Average percentage change for internal additive noise (i.e., additive noise) and external noise filtering (i.e., ext. noise filtering) PTM estimates ($n = 35$) with standard error of the mean as error bars.

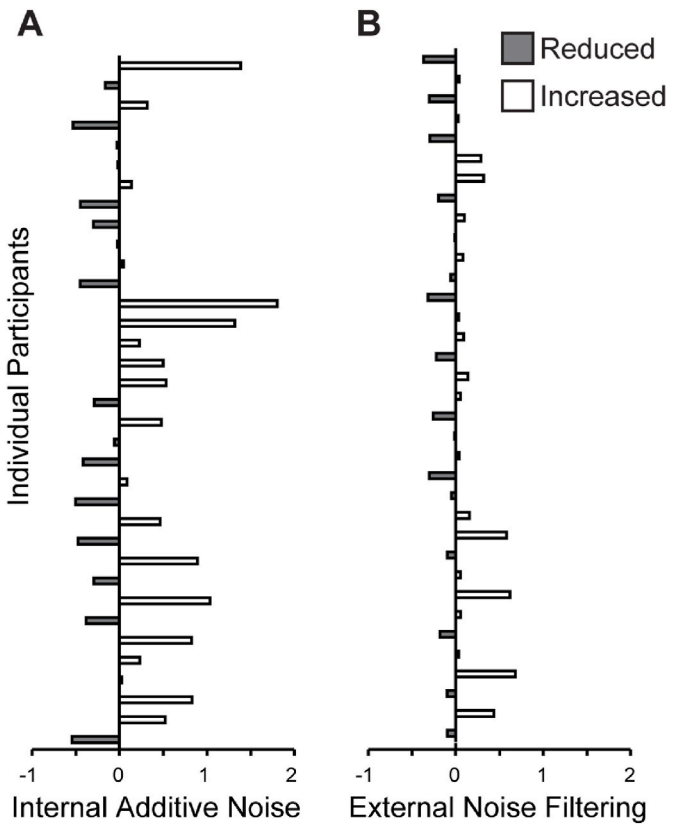

Fig. 4. Variability of hf-tRNS effects across individual participant PTM estimates.
Hf-tRNS effects across participants for A) internal additive noise and B) external noise filtering reflect the change in corresponding noise types under 3mA hf-tRNS relative to sham-tRNS conditions. A negative shift from zero is indicative of a reduction (n=16), while a positive shift is indicative of an increase (n=19) in each noise type. Note that an increase in external noise filtering estimates is indicative of poorer filtering.

for 3 mA hf-tRNS across low external noise levels compared to sham-tRNS (Fig. 3A). Ability to filter external noise was poorer for participants under 3 mA hf-tRNS conditions compared to sham-tRNS, as demonstrated by an average ~3% increase in external noise filtering estimates. This small difference was demonstrated as a slight increase in contrast thresholds across high external noise conditions in the TvN functions (Fig. 3A).[4] The meaningful deviation of model AF from the null model shown by AIC estimates indicates that changes in additive noise and external noise filtering meaningfully drive the differences in behavioural data seen between sham and active stimulation conditions.

PTM estimates across individual participants showed considerable variability (Fig.4A and B). Overall, 3 mA hf-tRNS appeared to increase internal additive noise and decreased the ability to filter external noise in ~55% of participants (Fig.4A and B, respectively). In order to explore whether baseline internal noise levels could explain the individual differences in noise estimates derived from the PTM, we used the slope parameter of each observer's psychometric function under sham conditions with zero external noise as a measure of baseline internal noise. As outlined by Aihara et al. (2010), the spread of the psychometric function corresponds to trial-to-trial variability, and therefore, is assumed to reflect the total noise level in the system. Accordingly, under the sham stimulation condition when zero external noise was applied, the spread of the psychometric function may be interpreted to reflect performance that is limited by the internal noise level alone. Independent samples *t*-test marginally showed that participants with 3 mA hf-tRNS-induced increases in internal additive noise appeared to generally have smaller slope estimates ($M = 2.16$, $SD = 0.09$) that is indicative of greater baseline internal noise relative to those with who presented reduction in internal additive noise ($M = 2.20$, $SD = 0.11$), $t(27.85) = 1.31$, $p = .100$. Taken at face value, this suggests that 3 mA hf-tRNS had a tendency to *increase* internal additive noise in observers with high baseline noise (but see discussion). With regards to external noise filtering, independent samples *t*-test showed no difference in slope estimates between 3 mA hf-tRNS-induced external noise filtering increased and reduced outcomes (Increased: $M = 2.19$, $SD = 0.03$, reduced: $M = 2.17$, $SD = 0.03$; $t(32.19) = -0.86$, $p = .395$).

4. Discussion

The present study provides evidence that high intensity (3 mA) hf-tRNS over V1 worsens perceptual performance across increasing external noise levels in a contrast detection task. Computational modelling using the PTM suggests that detrimental effects of tRNS on performance resulted from increased internal additive noise and reduced ability to filter external noise. No effects of 3 mA hf-tRNS were seen on internal multiplicative noise. Furthermore, analyses of individual differences offer tentative evidence suggesting that responses to 3 mA hf-tRNS may be determined by the baseline noise levels pre-existing in the observer's system. These findings provide important implications for the application of hf-tRNS as a means of investigating the impacts of noise on perception.

When considered in the context of pre-existing work, our result that 3 mA hf-tRNS can be detrimental to performance by increasing internal additive noise provides further evidence for SR as a plausible mechanism underlying hf-tRNS effects on performance. As discussed in the introduction, previous research only demonstrated one part of the SR effect, showing improved performance for low intensities of stimulation with hf-RNS and no change in performance with medium intensities (Van Der Groen and Wenderoth, 2016; Ghin et al., 2018; Pavan et al., 2019; O'hare et al., 2021; Battaglini et al., 2023, Potok et al., 2023). Recently, hf-tRNS was observed to negatively affect perception of higher-level perceptual features such as coherent motion, an effect that is, however, not attributed to increased internal noise (Pavan et al., 2019). Therefore, whether high amounts of internal noise detrimentally affect perception has not been tested in contrast detection tasks using hf-tRNS. Our findings therefore add the missing piece of information as predicted by SR, namely, that high intensities negatively affect perceptual performance by increasing additive noise.

Importantly, analyses of individual differences in the response to hf-tRNS demonstrated substantial variability across participants, with some participants showing improved perceptual performance at low levels of external noise. The PTM characterised such performance benefits as being due to a reduction in internal additive noise in response to 3 mA hf-RNS. This finding exposed limitations of the use of the PTM to index noise characteristics related to SR. In particular, the PTM assumes that increased internal noise will always result in detrimental effects to performance. Therefore, it simply cannot model improved performance that is due to SR. The PTM shares this limitation with similar approaches, such as the linear amplifier model, that has been shown to misestimate the level of internal noise, when conditions allow for SR (van Boxtel, 2019). This has serious implications when interpreting

[4] We would like to highlight that including all participants ($N = 41$) in this analysis resulted in larger averages for additive noise (42.3% increase) and external noise filtering (9% increase) model estimates compared to the screened sample ($n = 35$; See Appendix A, Fig A-1). The exclusion of 6 participants was based on poor model fits (See Appendix A, Table A-1). Even though the data of these 6 participants would have appeared to strengthen our results, we did not deem these data to be reliable, and therefore, the data we present after exclusions may be considered to be a conservative representation of our full sample. The excluded participants did not present any particular personal characteristics that could allow us to draw conclusions about why their data could not be modelled to a higher standard.

modelling results. Specifically, in the case of SR, improved performance is not necessarily due to reduced internal noise in the system, but rather, low to moderate *increases* in internal noise. Yet, the PTM would incorrectly attributed these changes in performance to a reduction of internal additive noise.

Our individual differences analysis provides tentative evidence in support of this perspective. We found a trending relationship where participants with low baseline internal noise levels were associated with improved perceptual performance under 3 mA hf-tRNS compared to sham, while high baseline internal noise levels related to negative effects in performance. This pattern of results is consistent with predictions by SR, where hf-tRNS may have pushed low baseline noise levels to the point at which neural noise improves perceptual performance. Conversely, for observers with higher pre-existing baseline noise levels, hf-tRNS may have increased neural noise beyond the optimal level and pushed it into the range of detrimental levels. While 3 mA hf-tRNS also appeared to have varying effects across observers' ability to filter external noise, individual baseline noise levels did not appear to explain this observation. Overall, these results are consistent with predictions by SR, and suggest that the PTM misestimates internal additive noise when the added system noise benefits performance. In a recent publication, Potok et al. (2023) were able to individualise tRNS stimulation for each participant by investigating performance under increasing current intensities to determine an 'optimal' current intensity that benefited performance. Future research could implement a similar protocol to reduce individual variability across a given sample, especially if interested in exploring detrimental effects of tRNS.

A similar explanation regarding the limits of the PTM to account for SR might be applicable to a previous study that found no performance changes in response to stimulation with 2 mA hf-tRNS (Melnick et al., 2020). Their PTM analysis suggested that such medium intensities do not modulate internal noise. However, it is also possible that the increased noise induced by 2 mA hf-tRNS may have resulted in performance that was equivalent to baseline performance, landing at the cross-over point between facilitative and suppressive effects on a SR curve. As PTM estimates are based on differences in perceptual performance between active and sham conditions, if there is no difference in performance between stimulation groups across low external noise conditions, the PTM attributes this finding to no change to the internal additive noise estimate. Thus, it is likely that internal additive noise did increase under 2 mA hf-tRNS. However, this effect was not visible as a *change* in performance and was therefore not detected by the PTM.

The results also indicate that exposure to 3 mA hf-tRNS generally diminished participant's ability to filter external noise. This is shown as a slight increase in contrast thresholds (i.e., worse performance) at higher external noise levels under 3 mA hf-tRNS compared to sham. This finding is inconsistent with another observation presented by Melnick and colleagues that demonstrated the opposite effect, i.e., improved external noise filtering effects from 2 mA hf-tRNS (Melnick et al., 2020). These results are most likely due to differences in our stimulation protocol, where we minimised the potential for the effects to be contaminated by adaptation by presenting stimulus-locked intermittent hf-tRNS. The inconsistent and changing environment produced by intermittent stimulation may have substantially reduced the possibility for adaption to occur, diminishing the observers' ability to filter external noise.

We recognise that a limitation of the present study is that we did not record participant sensation perceptions (e.g., headache, tingling, itching, heat, and pain) across sham and 3 mA hf-tRNS conditions, and that this may have impacted task performance. However, we note that data analysed from another study implementing a similar stimulation protocol (i.e., intermittent 3 mA hf-tRNS) did not identify any significant associations between sensation perceptions and perceptual performance (unpublished data, see supplementary material). We also recognise that we did not recruit a gender balanced sample, with the majority of the sample presenting as female. This could be problematic as females typically show lower cortical excitability compared to males, and therefore may be differently impacted by stimulation compared to males (Chaieb et al., 2008; Kuo et al., 2006). Although, cortical excitability appears matched for females and males during the follicular phase of the menstrual cycle (Inghilleri et al., 2004; Smith et al., 2002; Snowball et al., 2013). If we had controlled for this by testing females during the follicular phase of their menstrual cycle, the females in our sample may have been more likely to show the detrimental effects of hf-tRNS on perception. As discussed above, we propose that the addition of noise induced by hf-tRNS to a system that already has high baseline noise would more likely result in detrimental effects on performance (based on SR). Finally, while we have emphasised the non-monotonic effect of hf-tRNS on performance, we recognise that we have only tested one amplitude level in the present study. Comparatively, other published work tends to explore behavioural effects associated with increasing from weak to moderate current intensities (e.g., Van Der Groen and Wenderoth, 2016; Pavan et al., 2019). Our experimental design prioritised adequate data quantity to support the application of the PTM; because a considerable amount of data is needed for each external noise condition, the task was quite lengthy and demanding for participants. The 3 mA intensity was of primary interest to understand the potential detrimental effects of hf-tRNS. Therefore, the decision was taken to include a sham and single hf-tRNS intensity.

In conclusion, this study shows that visual performance can be detrimentally impacted by 3 mA hf-tRNS compared to sham. Modelling with the PTM suggests that the mechanisms driving this effect are increased internal additive noise and impaired external noise filtering. In the context of previous work, these results further support the notion that hf-tRNS increases additive noise to affect performance in line with SR. However, our findings, and in particular our individual differences analyses, also highlight an inherent limitation in using the PTM to capture noise characteristics related to SR.

Conflicts of interest

The authors declare no competing financial interests.

Research data

The data and codes supporting the findings of this study are available from the corresponding author upon reasonable request.

CRediT authorship contribution statement

Stephanie Gotsis: Conceptualization, Methodology, Software, Formal analysis, Investigation, Resources, Writing – original draft, Writing – review & editing, Project administration. **Jeroen J.A. van Boxtel:** Software, Formal analysis, Writing – review & editing. **Christoph Teufel:** Methodology, Writing – review & editing. **Mark Edwards:** Writing – review & editing. **Bruce K. Christensen:** Methodology, Writing – review & editing, Supervision.

Data availability

Data will be made available on request.

Acknowledgements

The present study was conducted while under a scholarship to support the completion of doctoral research (Australian Government Research Training Program (ARGTP) Stipend). The funders had no role in the study design, data collection and analysis, decision to publish, or preparation of the manuscript.

Appendix A

Table A1
Individual participant PTM estimates for the best fitting PTM determined with AIC for all participants (N=41).

	Model Estimates		Model Parameters					
ID	Aa	Af	N_{mul}	N_{add}	β	γ	R^2full	R^2red
1	0.457	0.904	0.000	0.000	3.026	3.383	0.754	0.712
2	1.521	1.434	0.000	0.000	2.289	4.420	0.754	0.629
3	1.829	0.901	0.126	0.000	1.264	5.955	0.956	0.950
4	1.023	1.682	0.015	0.000	3.036	3.833	0.690	0.545
5	1.233	1.031	0.001	0.000	2.717	3.606	0.851	0.850
6	0.183	1.082	0.000	0.001	1.854	3.399	0.482	0.411
7	0.035	1.757	0.012	0.000	2.032	6.067	0.484	0.268
8	1.825	0.819	0.006	0.000	2.211	2.908	0.792	0.763
9	0.615	1.055	0.000	0.000	2.248	3.626	0.904	0.897
10	2.034	1.620	0.001	0.000	2.108	3.582	0.637	0.558
11	0.825	1.377	0.000	0.004	5.942	3.902	0.392	0.363
12	0.706	1.051	0.006	0.000	2.759	4.190	0.877	0.870
13	1.890	0.902	0.000	0.000	2.455	3.006	0.795	0.777
14	0.524	1.579	0.013	0.000	1.718	4.931	0.929	0.862
15	1.465	1.157	0.001	0.000	2.106	3.876	0.850	0.834
16	0.495	0.951	0.001	0.000	2.488	4.114	0.679	0.649
17	1.083	0.696	0.000	0.000	2.191	3.217	0.794	0.745
18	0.581	1.038	0.000	0.000	2.490	3.121	0.850	0.838
19	0.944	0.985	0.000	0.001	2.302	2.754	0.784	0.784
20	1.479	0.741	0.000	0.000	1.924	3.196	0.822	0.789
21	0.261	2.044	0.000	0.001	2.181	3.485	0.639	0.439
22	0.713	1.051	0.002	0.000	1.942	3.158	0.902	0.899
23	1.532	1.137	0.018	0.000	1.544	3.323	0.860	0.851
24	1.497	0.777	0.007	0.000	2.267	3.864	0.773	0.750
25	1.226	1.088	0.000	0.001	2.728	2.578	0.796	0.790
26	2.317	1.030	0.009	0.000	2.354	4.537	0.864	0.833
27	1.749	1.057	0.133	0.000	1.140	7.617	0.412	0.401
28	2.801	0.683	0.000	0.001	2.194	2.727	0.609	0.558
29	0.547	0.940	0.000	0.001	3.421	3.189	0.773	0.735
30	1.046	1.079	0.000	0.000	2.630	3.428	0.724	0.722
31	0.975	0.987	0.000	0.000	2.386	3.315	0.865	0.864
32	0.701	1.098	0.001	0.000	2.928	4.339	0.640	0.633
33	0.552	0.802	0.000	0.000	2.502	3.764	0.604	0.535
34	1.136	1.316	0.004	0.000	2.567	4.266	0.940	0.906
35	13.586	1.458	0.033	0.000	3.056	4.591	0.648	0.412
36	0.981	1.285	0.000	0.004	4.290	2.506	0.684	0.656
37	0.970	0.703	0.000	0.000	2.016	3.185	0.650	0.606
38	0.469	1.027	0.049	0.000	1.726	5.425	0.886	0.872
39	1.317	0.697	0.000	0.000	2.031	3.384	0.898	0.838
40	0.838	1.041	0.002	0.000	2.212	3.872	0.932	0.931
41	2.387	0.630	0.056	0.000	2.038	4.679	0.829	0.724

Note. Model estimates: Aa = Internal additive noise, Af = External noise filtering; Model Parameters: N_{mul} = Multiplicative noise, N_{add} = Additive noise, β = beta, γ = gamma, R^2full = goodness of fit for the full PTM model including Aa and Af, R^2red = goodness of fit for the reduced model when Aa and Af are set to 1. Grey data is indicative of excluded participants based on poor model fitting; that is., data could not be modelled to a moderate or strong standard as indicated by R^2 values that fall below 0.5 (Moore et al., 2013).

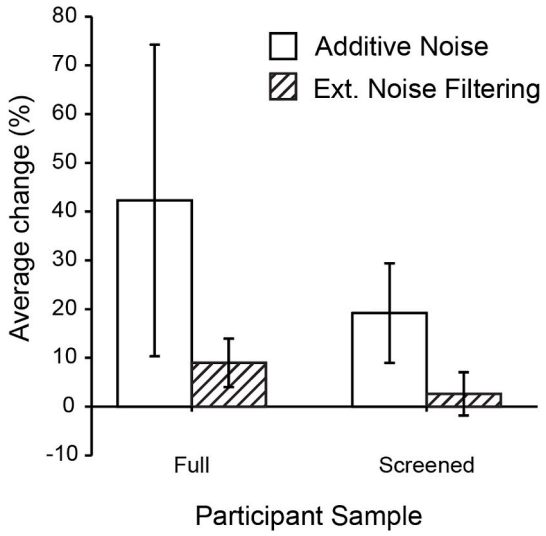

Fig. A-1. Perceptual template model percentage change in noise estimates for full and screened participant samples. The average percentage change for internal additive noise (i.e., additive noise; white) and external noise filtering (i.e., ext. noise filtering; striped) PTM estimates comparing 3mA hf-tRNS to sham for the full participant sample ($N = 41$) and the screened participant sample ($n = 35$).

Appendix B

AIC Model Selection for Individual Participants

Table B-1
Raw individual participant Akaike Information Criterion (AIC) estimates for PTM parameter combinations.

ID	Model Parameter Combinations							
	AFM	AF	AM	FM	A	F	M	NULL
1	-17.49	-19.49	-18.70	-14.62	-20.70	-16.46	-15.78	-15.97
2	-79.16	-81.16	-68.85	-78.12	-69.21	-79.77	-69.10	-65.44
3	-103.60	-105.62	-101.48	-104.84	-101.55	-106.75	-103.48	-103.35
4	-35.55	-37.44	-24.21	-37.54	-23.22	-39.43	-26.12	-23.03
5	-10.66	-12.66	-12.58	-12.30	-14.58	-14.30	-14.22	-16.18
6	-19.41	-21.41	-18.47	-18.00	-19.94	-19.19	-17.17	-19.17
7	-36.35	-38.35	-37.90	-36.34	-39.90	-37.43	-37.23	-39.22
8	18.90	17.05	23.10	18.38	22.27	16.38	21.99	22.47
9	-70.69	-72.69	-72.19	-70.80	-74.19	-72.36	-72.13	-74.06
10	-18.57	-20.57	-19.87	-16.95	-21.62	-18.94	-18.51	-20.51
11	-65.90	-67.90	-40.51	-64.75	-38.05	-66.22	-42.17	-39.93
12	-49.35	-51.35	-49.93	-50.03	-50.84	-51.47	-51.34	-50.63
13	-37.05	-39.05	-38.96	-36.31	-40.96	-38.31	-37.40	-38.83
14	-15.31	-17.31	-10.01	-17.26	-9.28	-19.26	-12.05	-11.08
15	-30.12	-32.12	-31.99	-28.37	-33.99	-30.34	-30.37	-32.34
16	-23.44	-25.44	-25.42	-25.41	-27.42	-27.41	-27.37	-29.37
17	-14.97	-16.97	-11.61	-15.50	-11.11	-17.50	-12.26	-12.77
18	-33.29	-35.09	-35.28	-33.84	-36.77	-35.84	-35.61	-37.59
19	-37.97	-39.65	-39.90	-39.73	-40.13	-40.36	-41.49	-40.85
20	-24.81	-26.81	-23.31	-25.49	-24.33	-27.49	-24.48	-26.16
21	-19.24	-21.24	-20.80	-20.60	-22.80	-22.60	-22.03	-23.99
22	-77.36	-79.36	-79.24	-71.84	-81.24	-73.27	-73.67	-73.40
23	-5.41	-7.41	-4.40	-2.98	-5.83	-4.84	-3.60	-5.55
25	-31.67	-33.67	-33.36	-28.25	-35.36	-30.06	-29.95	-30.20
25	-21.69	-23.69	-23.42	-23.67	-25.42	-25.67	-25.30	-27.30
26	-63.66	-65.66	-65.64	-65.65	-67.64	-67.65	-67.61	-69.61
27	-27.68	-29.68	-28.97	-29.09	-30.97	-31.09	-30.70	-32.70
28	-34.01	-36.01	-33.36	-32.63	-35.31	-34.60	-31.96	-32.27
29	-95.28	-97.28	-84.82	-96.98	-79.78	-98.79	-81.57	-79.82
30	-9.04	-11.04	-8.18	-11.03	-9.26	-13.03	-10.16	-10.97
31	-14.50	-16.50	-11.95	-16.50	-13.80	-18.50	-13.58	-14.80
32	-58.08	-60.07	-60.03	-55.21	-62.00	-56.59	-56.82	-58.56
33	-59.89	-61.89	-47.17	-60.60	-41.84	-62.60	-47.62	-43.82
34	-59.83	-61.83	-61.48	-61.28	-63.48	-63.27	-63.01	-65.01
35	-54.45	-56.45	-39.01	-51.93	-37.78	-51.61	-36.31	-37.45

Table B-2
Average Akaike Information Criterion (AIC) estimates and weight calculation for PTM parameter combinations for participants when model AF, model F, and the null has the best fit.

	Model Parameter Combinations							
	AFM	AF	AM	FM	A	F	M	Null
				AF (n=6)				
aveAIC	-43.06	-45.06	-34.10	-41.40	-34.35	-42.71	-33.39	-33.30
ΔAIC	2.00	0.00	10.96	3.66	10.71	2.35	11.67	11.76
w(AIC)	0.20	0.54	0.00	0.09	0.00	0.17	0.00	0.00
				F (n=11)				
aveAIC	-36.67	-38.65	-31.78	-37.94	-31.16	-39.86	-32.79	-32.18
ΔAIC	3.19	1.21	8.08	1.92	8.70	0.00	7.07	7.68
w(AIC)	0.09	0.25	0.01	0.17	0.01	0.45	0.01	0.01
				Null (n=8)				
aveAIC	-32.44	-34.41	-34.2	-33.98	-36.14	-35.98	-35.73	-37.72
ΔAIC	5.28	3.31	3.52	3.74	1.58	1.74	1.99	0.00
w(AIC)	0.03	0.07	0.06	0.05	0.16	0.15	0.13	0.35

Note. aveAIC = the average AIC estimate across participants with best fitting AF, F, and null models. ΔAIC is the difference between the best model and each other model; w(AIC) = is proportional to the total amount of predictive power provided by the full set of models contained in the model being assessed (Wagenmakers & Farrell, 2004). Perceptual Template Model parameter combinations: AFM – fullest model with Aa, Af, and Am coefficients free to vary; AF – Aa and Af coefficients free to vary; AM – Aa and Am coefficients free to vary; FM – Af and Am coefficients free to vary; A – Aa coefficient free to vary; F – Af coefficient free to vary; M – Am coefficient free to vary; Null – Aa, Af, and Am fixed to 1.

Appendix C. Supplementary data

Supplementary data to this article can be found online at https://doi.org/10.1016/j.neuropsychologia.2023.108703.

References

Aihara, T., Kitajo, K., Nozaki, D., Yamamoto, Y., 2010. How does stochastic resonance work within the human brain? – Psychophys. internal and external noise 375, 616–624. https://doi.org/10.1016/j.chemphys.2010.04.027.

Antal, A., Herrmann, C.S., 2016. Transcranial alternating current and random noise stimulation: possible mechanisms. Neural Plast. 2016, 1–12. https://doi.org/10.1155/2016/3616807.

Battaglini, L., Casco, C., Fertonani, A., Miniussi, C., Di Ponzio, M., Vicovaro, M., 2023. Noise in the brain: transcranial random noise stimulation and perceptual noise act on a stochastic resonance-like mechanism. Eur. J. Neurosci. 10, 433–436. https://doi.org/10.3389/fpsyg.2020.585437. Spatial vision.

Brainard, D.H., 1997. The Psychophysics Toolbox. Spatial Vision 10 (4), 433–436.doi. https://doi.org/10.1163/156856897X00357.

Chaieb, L., Antal, A., Paulus, W., 2008. Gender-specific modulation of short-term neuroplasticity in the visual cortex induced by transcranial direct current stimulation. Vis. Neurosci. 25 (1), 77–81. https://doi.org/10.1017/S0952523808080097.

Contemori, G., Trotter, Y., Cottereau, B.R., Maniglia, M., 2019. tRNS boosts perceptual learning in peripheral vision. Neuropsychologia 125, 129–136. https://doi.org/10.1016/j.neuropsychologia.2019.02.001.

Faisal, A.A., Selen, L.P., Wolpert, D.M., 2008. Noise in the nervous system. Nat. Rev. Neurosci. 9, 292–303. https://doi.org/10.1038/nrn2258.

Fertonani, A., Ferrari, C., Miniussi, C., 2015. What do you feel if I apply transcranial electric stimulation? Safety, sensations and secondary induced effects. Clin. Neurophysiol. : off. j. Int. Fed. Clin. Neurophysiol. 126 (11), 2181–2188, 0.1016/j.clinph.2015.03.015.

Fertonani, A., Miniussi, C., 2017. Transcranial electrical stimulation. Neuroscientist 23, 109–123. https://doi.org/10.1177/1073858416631966.

Ghin, F., Pavan, A., Contillo, A., Mather, G., 2018. The effects of high-frequency transcranial random noise stimulation (hf-tRNS) on global motion processing: an equivalent noise approach. Brain Stimul. 11 (6), 1263–1275. https://doi.org/10.1016/j.brs.2018.07.048.

Homayoun, H., Moghaddam, B., 2007. NMDA receptor hypofunction produces opposite effects on prefrontal cortex interneurons and pyramidal neurons. J. Neurosci. 27, 11496–11500. https://doi.org/10.1016/j.tins.2007.05.004.

Inghilleri, M., Conte, A., Currà, A., Frasca, V., Lorenzano, C., Berardelli, A., 2004. Ovarian hormones and cortical excitability. An rTMS study in humans. Clin. Neurophysiol. : off. j. Int. Fed. Clin. Neurophysiol. 115 (5), 1063–1068. https://doi.org/10.1016/j.clinph.2003.12.003.

Kleiner, M., Brainard, D., Pelli, D., 2007. What is new in Psychophysics Toolbox. Perception 36, 416. https://doi.org/10.1177/03010066070360S101.

Kuo, M.F., Paulus, W., Nitsche, M.A., 2006. Sex differences in cortical neuroplasticity in humans. Neuroreport 17 (16), 1703–1707. https://doi.org/10.1097/01.wnr.0000239955.68319.c2.

Lu, Z.-L., Dosher, B.A., 2008. Characterizing observers using external noise and observer models: assessing internal representations with external noise. Psychol. Rev. 115, 44. https://doi.org/10.1037/0033-295x.115.1.44.

McDonnell, M.D., Ward, L.M., 2011. The benefits of noise in neural systems: bridging theory and experiment. Nat. Rev. Neurosci. 12 (7), 415–425. https://doi.org/10.1038/nrn3061.

Melnick, M.D., Park, W.J., Croom, S., Chen, S., Batelli, L., Busza, A., Huxlin, K.R., Tadin, D., 2020. Online Transcranial Random Noise stimulation improves perception at high levels of visual white noise. bioRxiv. https://doi.org/10.1101/2020.06.22.165969.

Menzel, C., Hayn-Leichsenring, G.U., Redies, C., Németh, K., Kovács, G., 2017. When noise is beneficial for sensory encoding: noise adaptation can improve face processing. Brain Cognit. 117, 73–83. https://doi.org/10.1016/j.bandc.2017.06.006.

Miniussi, C., Harris, J.A., Ruzzoli, M., 2013. Modelling non-invasive brain stimulation in cognitive neuroscience. Neurosci. Biobehav. Rev. 37 (8), 1702–1712. https://doi.org/10.1016/j.neubiorev.2013.06.014.

Moore, D.S., Notz, W., Fligner, M.A., 2013. The Basic Practice of Statistics. WH Freeman, New York. https://doi.org/10.1080/00401706.1996.10484558.

Moss, F., Ward, L.M., Sannita, W.G., 2004. Stochastic resonance and sensory information processing: a tutorial and review of application. Clin. Neurophysiol. 115, 267–281. https://doi.org/10.1016/j.clinph.2003.09.014.

Neuling, T., Wagner, S., Wolters, C.H., Zaehle, T., Herrmann, C.S., 2012. Finite-element model predicts current density distribution for clinical applications of tDCS and tACS. Front. Psychiatr. 3, 83. https://doi.org/10.3389/fpsyt.2012.00083.

O'Hare, L., Goodwin, P., Sharp, A., Contillo, A., Pavan, A., 2021. Improvement in visual perception after high-frequency transcranial random noise stimulation (hf-tRNS) in those with migraine: an equivalent noise approach. Neuropsychologia 161, 107990. https://doi.org/10.1016/j.neuropsychologia.2021.107990.

Pavan, A., Ghin, F., Contillo, A., Milesi, C., Campana, G., Mather, G., 2019. Modulatory mechanisms underlying high-frequency transcranial random noise stimulation (hf-tRNS): a combined stochastic resonance and equivalent noise approach. Brain Stimul. 12 (4), 967–977. https://doi.org/10.1016/j.brs.2019.02.018.

Pelli, D.G., Vision, S., 1997. The VideoToolbox software for visual psychophysics: transforming numbers into movies. Spatial Vis. 10, 437–442. https://doi.org/10.1163/156856897x00366.

Penton, T., Bate, S., Dalrymple, K.A., Reed, T., Kelly, M., Godovich, S., Tamm, M., Duchaine, B., Banissy, M.J., 2018. Using high frequency transcranial random noise stimulation to modulate face memory performance in younger and older adults: lessons learnt from mixed findings. Front. Neurosci. 12 https://doi.org/10.3389/fnins.2018.00863.

Potok, W., Post, A., Beliaeva, V., Bächinger, M., Cassarà, A.M., Neufeld, E., Polania, R., Kiper, D., Wenderoth, N., 2023. Modulation of visual contrast sensitivity with tRNS across the visual system, evidence from stimulation and simulation. eNeuro 10 (6). https://doi.org/10.1523/ENEURO.0177-22.2023.

Prins, N., Kingdon, F., 2009. Palamedes: Matlab Routines for Analyzing Psychophysical Data. www.palamedestoolbox.org.

Raul, P., McNally, K., Ward, L.M., van Boxtel Jja, 2023. Does stochastic resonance improve performance for individuals with higher autism-spectrum quotient? Apr 14 Front. Neurosci. 17, 1110714. https://doi.org/10.3389/fnins.2023.1110714.

Smith, M.J., Adams, L.F., Schmidt, P.J., Rubinow, D.R., Wassermann, E.M., 2002. Effects of ovarian hormones on human cortical excitability. Ann. Neurol. 51 (5), 599–603. https://doi.org/10.1002/ana.10180.

Snowball, A., Tachtsidis, I., Popescu, T., Thompson, J., Delazer, M., Zamarian, L., Zhu, T., Cohen Kadosh, R., 2013. Long-term enhancement of brain function and cognition using cognitive training and brain stimulation. Curr. Biol. : CB 23 (11), 987–992. https://doi.org/10.1016/j.cub.2013.04.045.

Treviño, M., De la Torre-Valdovinos, B., Manjarrez, E., 2016. Noise improves visual motion discrimination via a stochastic resonance-like phenomenon. Front. Hum. Neurosci. 10, 572. https://doi.org/10.3389/fnhum.2016.00572.

van Boxtel, J.J., 2019. Modeling stochastic resonance in humans: the influence of lapse rate. J. Vis. 19 https://doi.org/10.1167/19.13.19, 19-19.

Van Der Groen, O., Wenderoth, N., 2016. Transcranial random noise stimulation of visual cortex: stochastic resonance enhances central mechanisms of perception. J. Neurosci. 36, 5289–5298. https://doi.org/10.1523/jneurosci.4519-15.2016.

van der Groen, O.T., Wenderoth N, M.F., Mattingley, J.B., 2018. Stochastic resonance enhances the rate of evidence accumulation during combined brain stimulation and perceptual decision making. PLOS Comupt. Biol. https://doi.org/10.1371/journal.pcbi.1006301.

Wagenmakers, E.-J., Farrell, S., 2004. AIC model selection using Akaike weights. Psychonomic Bull. Rev. 11, 192–196. https://doi.org/10.3758/bf03206482.

Ward, L.M., 2009. Physics of neural synchronisation mediated by stochastic resonance. Contemp. Phys. 50 (5), 563–574. https://doi.org/10.1080/00107510902879246.